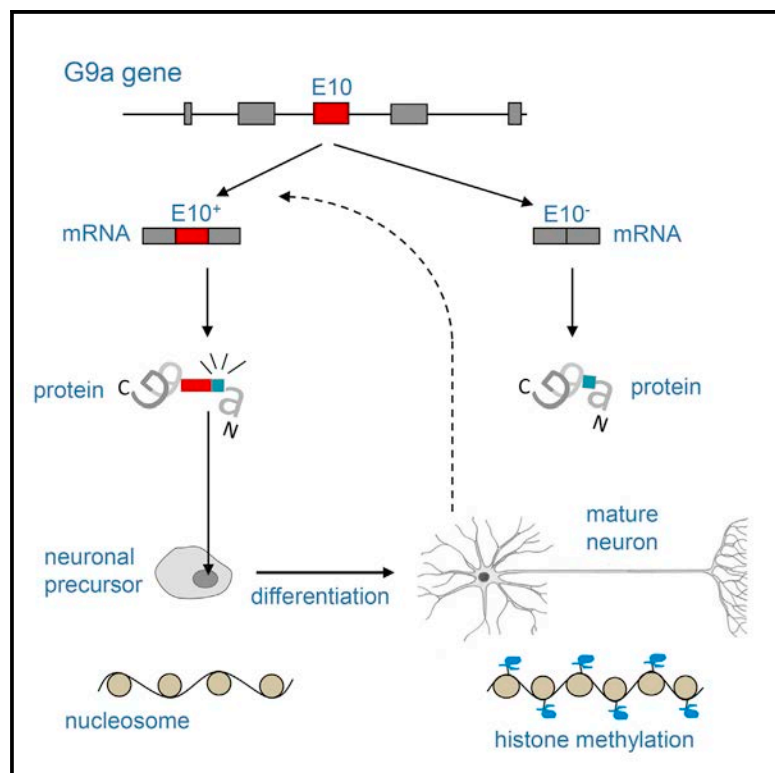


Alternative Splicing of G9a Regulates Neuronal Differentiation

Graphical Abstract



Authors

Ana Fiszbein, Luciana E. Giono,
Ana Quaglino, ..., Julio J. Caramelo,
Anabella Srebrow, Alberto R. Kornblihtt

Correspondence

ark@fbmc.fcen.uba.ar

In Brief

Fiszbein et al. show that the histone methyltransferase G9a regulates alternative splicing of its own transcript, an event critical for neuron differentiation. Inclusion of exon 10 stimulates H3K9me2 levels and promotes nuclear localization of G9a, creating a positive feedback loop that reinforces the cellular commitment to differentiation.

Highlights

- G9a is required for neuron differentiation
- Exon 10 inclusion in G9a is upregulated during neuron differentiation
- Inclusion of E10 promotes G9a nuclear localization
- G9a regulates its own alternative splicing through a positive feedback loop



Alternative Splicing of G9a Regulates Neuronal Differentiation

Ana Fiszbein,¹ Luciana E. Giono,¹ Ana Quaglino,¹ Bruno G. Berardino,² Lorena Sigaut,³ Catalina von Bilderling,³ Ignacio E. Schor,^{1,7} Juliana H. Enrique Steinberg,⁴ Mario Rossi,⁴ Lía I. Pietrasanta,^{3,5} Julio J. Caramelo,^{2,6} Anabella Srebrow,¹ and Alberto R. Kornblith^{1,*}

¹Departamento de Fisiología, Biología Molecular y Celular, Facultad de Ciencias Exactas y Naturales, Universidad de Buenos Aires and Instituto de Fisiología, Biología Molecular y Neurociencias (IFIBYNE-CONICET), Ciudad Universitaria Pabellón II, C1428EHA Buenos Aires, Argentina

²Departamento de Química Biológica, Facultad de Ciencias Exactas y Naturales, Universidad de Buenos Aires, Ciudad Universitaria Pabellón II, C1428EHA Buenos Aires, Argentina

³Departamento de Física, Facultad de Ciencias Exactas y Naturales, Universidad de Buenos Aires and IFIBA-CONICET, Ciudad Universitaria Pabellón I, C1428EHA Buenos Aires, Argentina

⁴Instituto de Investigación en Biomedicina de Buenos Aires CONICET, Partner Institute of the Max Planck Society, C1425FQD Buenos Aires, Argentina

⁵Centro de Microscopías Avanzadas, Facultad de Ciencias Exactas y Naturales, Universidad de Buenos Aires, Ciudad Universitaria, C1428EHA Buenos Aires, Argentina

⁶Fundación Instituto Leloir, C1405BWE Buenos Aires, Argentina

⁷Present address: Genome Biology Unit, European Molecular Biology Laboratory, 69117 Heidelberg, Germany

*Correspondence: ark@fbmc.fcen.uba.ar

<http://dx.doi.org/10.1016/j.celrep.2016.02.063>

This is an open access article under the CC BY-NC-ND license (<http://creativecommons.org/licenses/by-nc-nd/4.0/>).

SUMMARY

Chromatin modifications are critical for the establishment and maintenance of differentiation programs. G9a, the enzyme responsible for histone H3 lysine 9 dimethylation in mammalian euchromatin, exists as two isoforms with differential inclusion of exon 10 (E10) through alternative splicing. We find that the G9a methyltransferase is required for differentiation of the mouse neuronal cell line N2a and that E10 inclusion increases during neuronal differentiation of cultured cells, as well as in the developing mouse brain. Although E10 inclusion greatly stimulates overall H3K9me2 levels, it does not affect G9a catalytic activity. Instead, E10 increases G9a nuclear localization. We show that the G9a E10⁺ isoform is necessary for neuron differentiation and regulates the alternative splicing pattern of its own pre-mRNA, enhancing E10 inclusion. Overall, our findings indicate that by regulating its own alternative splicing, G9a promotes neuron differentiation and creates a positive feedback loop that reinforces cellular commitment to differentiation.

INTRODUCTION

The hundreds of different cell types found in multicellular organisms show vast differences in phenotype, function, and response to external stimuli, yet they all derive from the same zygotic cell and share identical genetic material. This diversity arises as a result of a complex and stepwise differentiation process that re-

quires activation and inactivation of transcriptional programs. In addition to specific sets of transcription factors, it has become clear that histone and DNA modifications are critical for both establishment of differentiation programs and maintenance of acquired differentiated phenotypes (Surani et al., 2007). Covalent modification of histone tails proved to be a convergent point of multiple signaling pathways and to embody an additional code superimposed on the genetic code (Bannister and Kouzarides, 2011; Jenuwein and Allis, 2001).

G9a, also known as EHMT2 (euchromatic histone lysine N-methyltransferase 2) and KMT1C (lysine methyltransferase 1C), is the enzyme responsible for H3K9 mono- and dimethylation (H3K9me1 and H3K9me2) in mammalian euchromatin and is essential for early mouse development (Tachibana et al., 2002). Mammals possess only one paralog of G9a, called GLP or EHMT1/KMT1D. Both enzymes are characterized by a C-terminal catalytic SET domain preceded by ankyrin repeats that function as mono- and dimethyllysine binding modules (Collins et al., 2008). G9a and GLP interact through their SET domains and are thought to function primarily as a heteromeric complex *in vivo* (Liu et al., 2015; Ohno et al., 2013). G9a knockout mice are embryonic lethal, and the derived embryonic stem cells show dramatically reduced levels of H3K9me1 and H3K9me2, histone marks that are generally associated with transcriptional silencing (Kramer, 2015). In particular, many non-histone targets of methylation by G9a have been described (Rathert et al., 2008), including p53 (Huang et al., 2010) and G9a itself, by automethylation (Chin et al., 2007).

G9a has been implicated in the differentiation of a variety of cell and tissue types. G9a is essential for the differentiation and growth of tendonocytes, with the expression of several tendon transcription factors being suppressed in G9a null cells (Wada et al., 2015). Furthermore, G9a cooperates with Sharp-1, a potent repressor of skeletal muscle differentiation, methylating

MyoD and histones at the myogenin gene promoter (Ling et al., 2012); G9a deficiency impairs differentiation of monocytes (Wierda et al., 2015) and T helper cells (Lehnertz et al., 2010).

In the nervous system, G9a has been shown to control cognition and adaptive responses by repression of nonneuronal genes (Schaefer et al., 2009). Its ortholog in *Drosophila* has been described as a regulator of peripheral dendrite development, classic learning, and memory genes (Kramer et al., 2011). Moreover, G9a has been shown to influence neuronal subtype specification (Maze et al., 2014) and regulate ethanol-induced neurodegeneration (Subbanna et al., 2013).

Alternative splicing not only is the most important source of mRNA and protein diversity but also greatly contributes to tissue- and species-specific protein patterns in multicellular eukaryotes (Barbosa-Morais et al., 2012; Ellis et al., 2012; Kornblhtt et al., 2013). Alternative splicing plays a role in a vast array of normal and pathological processes including cell proliferation and differentiation, as well as cancer and numerous diseases (Cáceres and Kornblhtt, 2002; Faustino and Cooper, 2003; Klemen et al., 2013; Liu et al., 2012). Pre-mRNA splicing commitment occurs mostly co-transcriptionally, but the actual splicing reaction can occur either co- or post-transcriptionally (Tilgner et al., 2012; Vargas et al., 2011). Co-transcriptional regulation allows for mechanistic interactions between the transcription and splicing machineries (Bentley, 2005; Kornblhtt et al., 2013; Neugebauer, 2002; Perales and Bentley, 2009).

Accumulating evidence points to the existence of multiple functional links between chromatin structure and pre-mRNA splicing (Luco et al., 2010; Naftelberg et al., 2015). Early reports with virus and plasmid systems (Adami and Babiss, 1991; Kadener et al., 2001) and more recent ones with endogenous genes show that several histone marks deployed intragenically are asymmetrically distributed between exons and introns (Kolasinska-Zwierz et al., 2009) and modulate alternative splicing decisions (Alló et al., 2009, 2014; Ameyar-Zazoua et al., 2012; Batsché et al., 2006; Schor et al., 2009, 2013). In addition to changes in the RNA polymerase II (RNAPII) elongation properties, chromatin marks can regulate both constitutive and alternative splicing by recruitment of splicing factors to transcription sites (Gonzalez et al., 2015; Luco et al., 2010; Sims et al., 2007). Using an RNAi-based screen targeting chromatin modifying proteins, Salton and colleagues have recently identified G9a as a major regulator of VEGFA alternative splicing (Salton et al., 2014). The mechanism involves intragenic H3K9 methylation at the VEGFA locus, recruitment of the heterochromatin protein HP1, and the splicing factor SRSF1, consistent with previous reports linking HP1 gamma to alternative splicing (Saint-André et al., 2011). The authors demonstrated separate roles for G9a in transcription and alternative splicing.

Here, we report that G9a is required for neuron differentiation and that this process correlates with increased inclusion of G9a alternative exon 10 (E10). Although E10 inclusion does not affect G9a intrinsic catalytic activity, it results in increased H3K9me2 levels due higher nuclear localization of the enzyme and appears to be necessary for efficient differentiation. The alternatively spliced exon does not encode a nuclear localization signal (NLS), but it is predicted to enhance the exposure of the neighboring constitutive NLS to the external hydrophilic milieu. More-

over, G9a regulates its own alternative splicing, suggesting a positive feedback loop that upregulates H3K9me2 during cell differentiation.

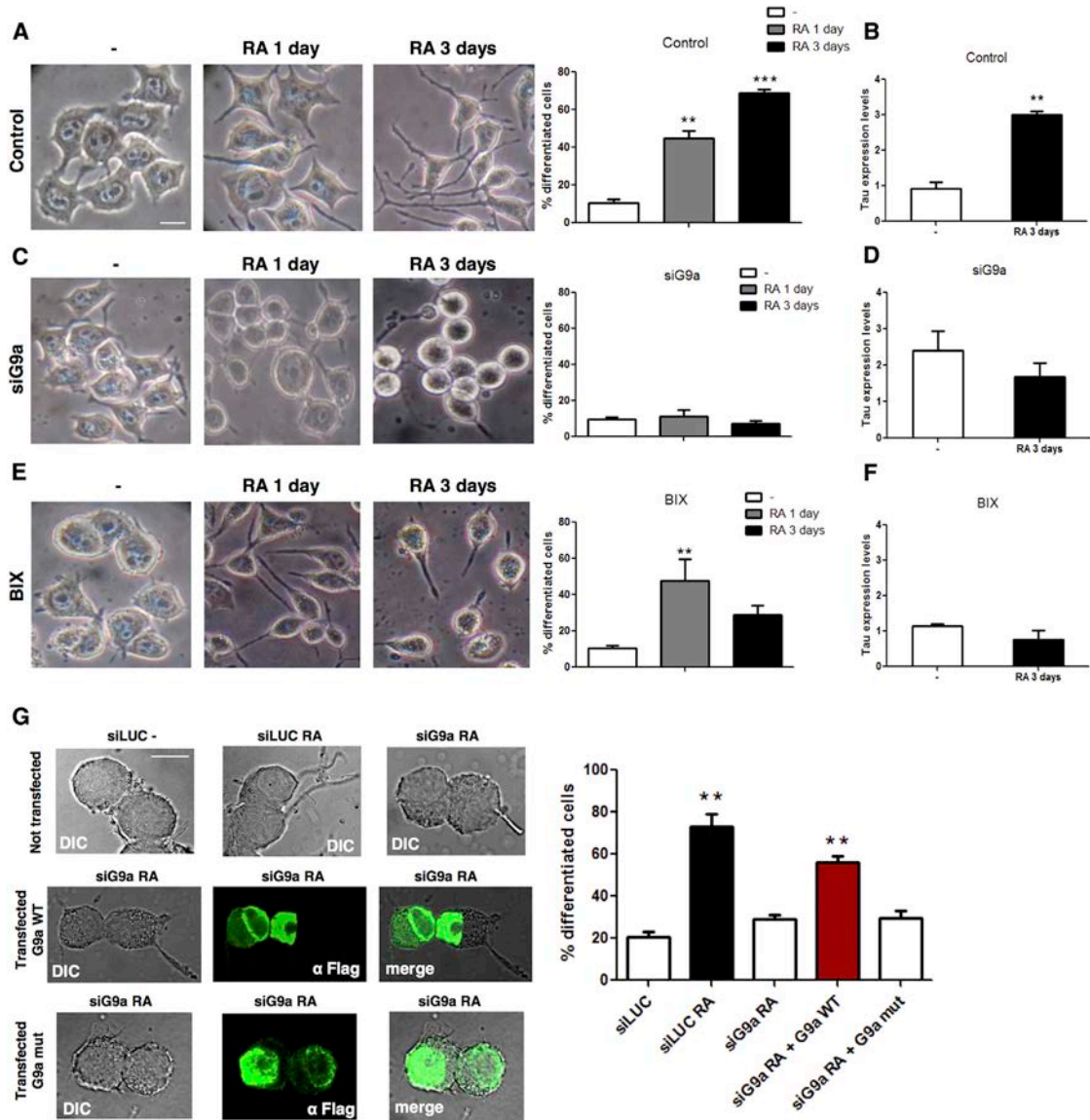
RESULTS

G9a Is Required for Neuron Differentiation

The euchromatin histone methyltransferase G9a has been reported to affect the differentiation process of a variety of cells and tissues. Here, we used a well-established model of neuronal differentiation to study the role of G9a during the differentiation of precursors cells into mature neurons. Neuro 2a (N2a) is a mouse-neural-crest-derived cell line that can be differentiated into neurons and has been extensively used to study neuronal differentiation. N2a cells treated with 1 μM retinoic acid (RA) for 1–3 days readily enter a differentiation program as reflected by neurite sprouting (Figure 1A) and the increased expression of Tau (microtubule-associated protein tau), a specific neuronal marker (Figure 1B). Depletion of G9a in N2a using small interfering RNA (siRNA) prior to the differentiation treatment completely abolishes both neurite outgrowth (Figure 1C) and the upregulation of Tau expression (Figure 1D). BIX-01294 (BIX) is a diazepin-quinazolin-amine derivative that selectively inhibits G9a and GLP methyltransferase activities and has been shown to reduce overall H3K9me2 levels in several cell types (Chang et al., 2009; Kubicek et al., 2007; Shi et al., 2008). N2a cells treated with BIX from the initiation of the differentiation protocol begin to develop neurites but fail to fully establish and maintain the differentiated phenotype compared to control cells (Figure 1E). Moreover, BIX treatment completely abolishes the increase in Tau expression during differentiation (Figure 1F). These results confirm a role for G9a and its histone methyltransferase activity in the differentiation of N2a cells into neurons. To reinforce this conclusion, the abolishment of neurite outgrowth in G9a knockdown cells can be rescued by transfecting the cells with an expression construct encoding the human wild-type G9a, but not with its catalytically dead mutant counterpart (Figure 1G), strongly indicating that the effect depends on G9a enzymatic activity.

G9a Pre-mRNA Is Alternatively Spliced during Neuron Differentiation

Both in humans and mice, G9a mRNA has two isoforms resulting from alternative splicing of its exon 10 (E10) (Brown et al., 2001). Although it inserts an internal segment of 33 amino acids toward the NH₂-terminal third of the protein, inclusion of E10 does not alter the reading frame of G9a mRNA, neither does it affect any characterized domain of the protein (Figure 2A). G9a E10 inclusion increases when N2a cells are subjected to the DMSO differentiation protocol (Figure 2B). The same upregulation is observed with the differentiation protocol that uses RA (Figure 2C) and in a different cell line, P19, in which mouse embryonic stem cells are induced to form embryonic bodies and later neural cells (Figure 2D). Most importantly, E10 inclusion is upregulated in whole brains from newborn mice from postnatal days 1–7 and is maintained significantly elevated for as long as 4 months after birth (Figure 2E). This regulation is not restricted to neuron differentiation, since during T cell stimulation (Martinez

**Figure 1. G9a Is Required for Neuron Differentiation**N2a cells were differentiated by treatment with 1 μ M RA for 1–3 days.

(A and B) The percentage of cells displaying neurite outgrowth (differentiated cells) was determined (A), and mRNA levels of the neuronal marker Tau was assessed (B) by qRT-PCR and relativized using HSPCB (heat shock protein class B) as a housekeeping.

(C–F) N2a cells were transfected with G9a siRNA (siG9a) (C and D) or treated with 3 μ M BIX (E and F) previously to differentiation induction and analyzed as described in (A) and (B).

(G) Prior to differentiation induction, N2a cells were cotransfected with siG9a or luciferase siRNA (siLUC) as a control, together with rescue plasmids encoding human Flag-tagged G9a full-length wild-type (WT) or catalytically dead mutant (mut) cDNAs. The expression of these human constructs is not downregulated by the mouse G9a siRNAs used here and along the report. Cells were fixed and Flag-tagged G9a expression was assessed by indirect immunofluorescence. In view of the higher efficiency of siRNA transfection compared to the plasmid transfection, differentiation was only assessed in the cells showing positive fluorescence. The plot on the right shows the percentage of differentiated cells.

Scale bars represent 10 μ m. Statistical analysis corresponds to one-way ANOVA, Bonferroni post hoc test (** $p < 0.001$, and *** $p < 0.0001$).

et al., 2012) and mammary gland differentiation, E10 inclusion is also increased (Figure 2F).

E10 Inclusion Is Required for Neuron Differentiation

Since G9a is required for neuron differentiation and E10 inclusion is upregulated in mature neurons, we sought to determine if E10

inclusion in G9a is responsible for promoting neuron differentiation. For this, we knocked down the E10-containing mRNA isoform using an siRNAs specifically targeting E10 sequence (siE10). Under conditions in which total amounts of G9a mRNA (Figure S1A) and protein (Figure S1B) levels are not affected, siE10 reduces the levels of the E10⁺ G9a mRNA isoform in N2a

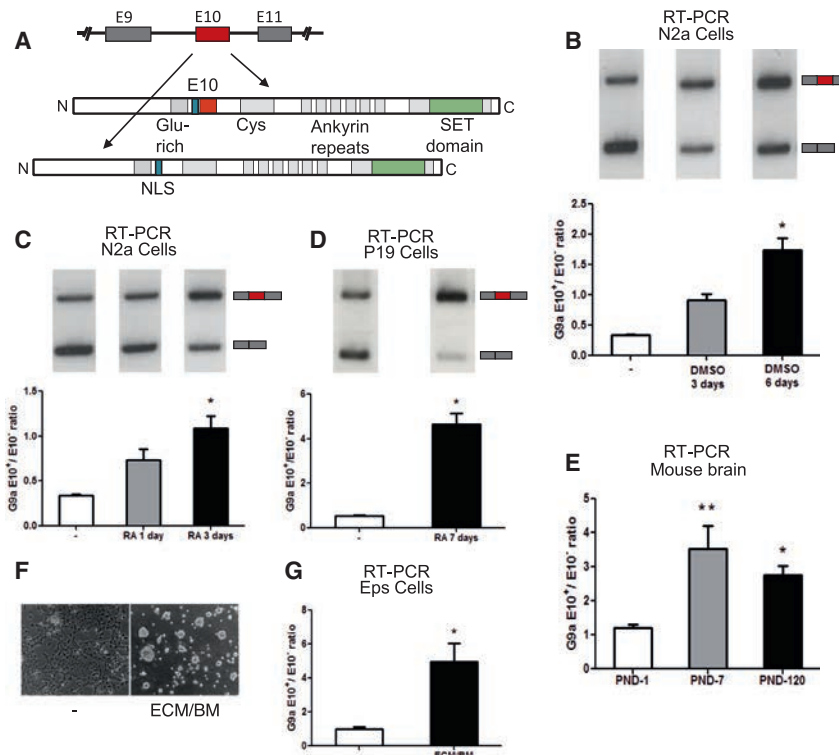


Figure 2. Alternative Splicing of G9a Gene Is Modulated during Neuron Differentiation

(A) Schematic diagram of the G9a gene showing the alternatively spliced isoforms containing and lacking E10.

(B and C) N2a cells were differentiated with 2% DMSO (B) or 1 μ M RA (C) for 1 to 6 days. At the indicated time points, cells were harvested, RNA was extracted, and alternative splicing of the G9a gene was assessed by radioactive RT-PCR.

(D) P19 cells were differentiated with RA for 7 days and alternative splicing of G9a was assessed as described. RT-PCR gels are shown at the top and the corresponding quantification at the bottom.

(E) Mouse brains were sampled at postnatal day (PND) 1, 7, and 120. RNA was extracted, and alternative splicing of G9a was assessed as described.

(F) Mammary epithelial cells were differentiated with extracellular matrix (ECM) and basal membrane (BM) in presence of lactogenic hormones as described in [Experimental Procedures](#). Cells were harvested, RNA was extracted, and alternative splicing of the G9a gene was assessed as described. The corresponding quantification is shown on the right.

All experiments were performed in triplicate, and means and SE of representative experiments are shown. Statistical analysis corresponds to one-way ANOVA, Bonferroni post hoc test (*p < 0.05 and **p < 0.001).

cells treated with RA (Figure 3A). The siE10 treatment causes a significant inhibition of differentiation (Figures 3B and C), revealing that inclusion of E10 has an crucial role in the promotion of neuron differentiation by G9a.

H3K9me2 Is Increased during Neuron Differentiation and Stimulated by E10 Inclusion

As we observed that G9a methyltransferase activity is required for neuron differentiation, we sought to evaluate the H3K9me2 global levels in precursor and mature neural cells. After 3 days of neuron differentiation induced by RA, N2a cells present a significantly stronger signal of H3K9me2 compared to undifferentiated cells (Figure 4A). As neuron differentiation correlates with H3K9me2 upregulation and G9a E10 inclusion, we decided to analyze the effect of E10 inclusion on G9a methyltransferase activity. For this, we transfected expression vectors encoding the two G9a isoforms (E10⁺ and E10⁻) into G9a clustered regularly interspaced short palindromic repeats (CRISPR)-ablated HEK293 cells and analyzed the global H3K9me2 levels. Figure 4B shows that H3K9 dimethylation is almost completely abolished in the G9a knockout cells (compare lanes 1 and 2). Overexpression of both G9a splicing isoforms partially rescue K9 dimethylation, with a stronger effect caused by the E10⁺ G9a variant (compare lanes 3 and 4). These results suggest that inclusion of E10 stimulates G9a's ability to methylate histone targets.

Exon 10 Inclusion Does Not Affect G9a Intrinsic Catalytic Activity

To further examine the role of E10 inclusion on G9a activity, we used a powerful methyltransferase fluorescence resonance

energy transfer (FRET) reporter (Lin et al., 2004). In this system, a peptide substrate corresponding to the K9 methylation site of histone H3 is joined via a flexible linker to a methyllysine binding domain known as a chromodomain. Upon methylation of the K9 residue, the chromodomain forms an intramolecular complex with the methyllysine side chain, altering the spatial relationship between flanking CFP and YFP units and changing the FRET level (Figure 4C). In order to obtain results that were independent from the subcellular localization of both the FRET sensor and the G9a splicing isoforms, fluorescence data were collected only from nuclear compartments of cells and relativized to expression levels of the E10⁻ or E10⁺ isoforms. Using this assay, both isoforms display similar methyltransferase abilities (Figure 4D), indicating that E10 inclusion does not stimulate G9a catalytic activity. This observation suggests that the increase in H3K9me2 levels elicited by E10 inclusion must be caused by a mechanism different from an increase in G9a intrinsic activity.

Exon 10 Inclusion Promotes G9a Nuclear Localization

The amino acid sequence encoded by E10 does not contain any NLS or any other recognizable consensus for specific functions. However, a bona fide bipartite NLS is located nine residues toward the N terminus from the start of the E10-encoded segment. Since the E10 protein sequence and the neighboring NLS are predicted by IUPred (Dosztányi et al., 2005) to be intrinsically unstructured, the inclusion of E10 places G9a's NLS in a more extended unstructured region (Figure 4E). Therefore, the disorder tendency of E10 could allow a structural arrangement that modulates the accessibility of the contiguous NLS. In view of

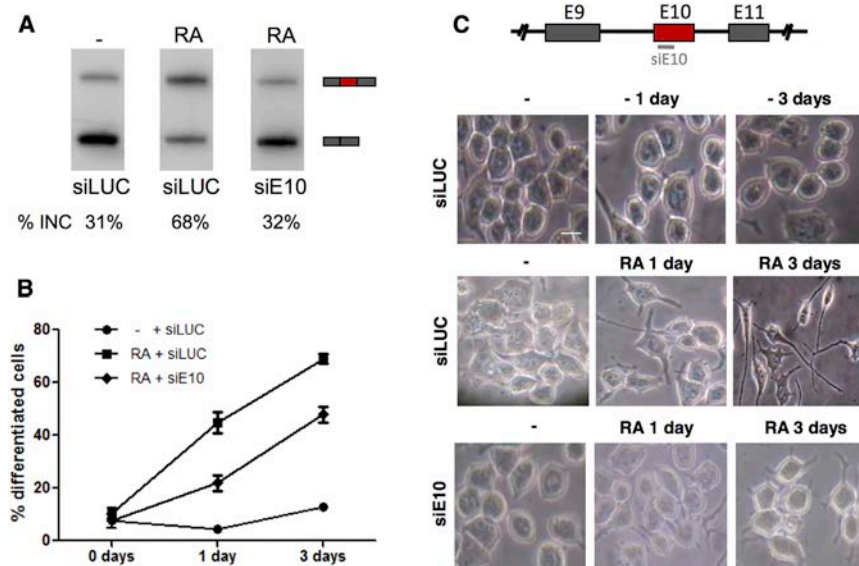


Figure 3. E10 Inclusion Is Required for Neuron Differentiation

N2a cells were differentiated by treatment with 1 μM RA (RA) or maintained undifferentiated (−) for 1–3 days and transfected with siLUC as a control or G9a E10 siRNA (siE10) previously to differentiation induction.

(A) Alternative splicing of G9a was assessed as described in Figure 2, and the percentage of E10 inclusion is indicated to show the effect of the siE10 treatment.

(B and C) The percentage of cells displaying neurite outgrowth was determined morphologically (B) and quantified (C). Scale bars represent 10 μm. A schematic diagram of G9a gene showing the target site of siE10 is shown (B, top). See also Figure S1.

this, we explored the possibility that E10 inclusion regulates the subcellular localization of G9a.

Immunofluorescence of N2a cells with an anti G9a antibody reveals cells with distinctive patterns. In undifferentiated cells, G9a is detected both in the nucleus and the cytoplasm. This pattern changes radically during neuron differentiation to an almost only nuclear localization (Figure 5A). Quantifications of the relative concentration of fluorescence intensity either using DMSO (Figure 5B) or RA (Figure 5C) indicate that neuron differentiation significantly increases the nucleus/cytoplasm ratio. The same results are obtained by quantifying the total fluorescence intensity in both cell lines (Figures S2A and S2B). Interestingly, there is a positive linear correlation between the degree of G9a E10 inclusion and the nuclear localization of G9a proteins in four different human cell lines analyzed (Figure S2C).

In order to obtain independent evidence, we assessed G9a localization by western blot in nuclear and cytoplasmic fractions of undifferentiated and differentiated N2a cells. Figure 5D shows that upon differentiation, the two protein isoforms differing by E10 decrease in the cytoplasmic fraction (compare overall intensities in lanes 1 and 3) and increase in the nuclear fraction (compare overall intensities in lanes 2 and 4). Furthermore, the nuclear fractions (lanes 2 and 4) display a higher E10⁺/E10[−] protein isoform ratios.

In view of results in Figure 5A and the observed increase in E10 inclusion into G9a mRNA upon differentiation (Figure 2), we reasoned that if E10 inclusion promotes the nuclear localization of the protein, G9a translocation to the nucleus should be impaired by siE10 treatment. In order to test this hypothesis, we analyzed the subcellular localization of G9a in N2a undifferentiated cells transfected with siE10. When comparing the relative concentration of G9a fluorescence intensity, siE10-treated cells show a nucleus/cytoplasm localization ratio significantly lower than control cells (Figure 5E).

To better determine whether E10 inclusion only correlates with or instead causes G9a nuclear localization, we transiently ex-

pressed Flag-tagged cDNAs encoding G9a with and without E10 in HeLa and N2a cells. Recombinant G9a displays two expression patterns in both cell types: only nuclear (n) or nuclear and cytoplasmic (n+c) (Figures 6A and 6B). At equal expression levels, verified by western blot (Figure 6C), expression of the E10⁺ isoform decreases the percentage of cells with the n+c pattern and increases the percentage of cells with the n pattern, both in HeLa (Figure 6D) and N2a cells (Figure 6E). This indicates that inclusion of E10 promotes the nuclear localization of the protein complexes that contain the G9a polypeptide.

G9a Regulates Alternative Splicing of Its Own Pre-mRNA through a Positive Feedback Loop

Extended evidence has revealed that chromatin modifications can affect alternative splicing (Saint-André et al., 2011; Salton et al., 2014; Schor et al., 2013; Shukla et al., 2011), and we have shown here that E10 inclusion correlates with increased nuclear localization of G9a and H3K9me2 levels. We therefore hypothesized that G9a might regulate its own alternative splicing.

Treating N2a differentiated cells with the K9 methylation inhibitor BIX completely reverts the increase in E10 inclusion triggered by neuron differentiation (Figure 7A). Although BIX prevents neuronal precursors to differentiate into mature neurons, in this case, the cells were treated after the differentiation program was already established in order to rule out a possible inhibition of differentiation. Indeed, BIX does not revert differentiation when already established (Figure S3). This observation supports the idea that G9a methyltransferase activity is required for the regulation of its own splicing during neuron differentiation.

An immediate question emerged whether upregulation of E10 inclusion could result from changes in H3K9 methylation on the G9a gene. Chromatin immunoprecipitation experiments show that neuronal differentiation increases H3K9me2 in the G9a gene body but not at the promoter or at a distant intergenic region (Figure S4A). As the upregulation of E10 inclusion correlates with increased H3K9me2 levels in G9a gene, we decided to analyze if chromatin structure plays a role in the regulation of G9a alternative splicing. The cytosine analog 5-azacytidine (5aC) and the

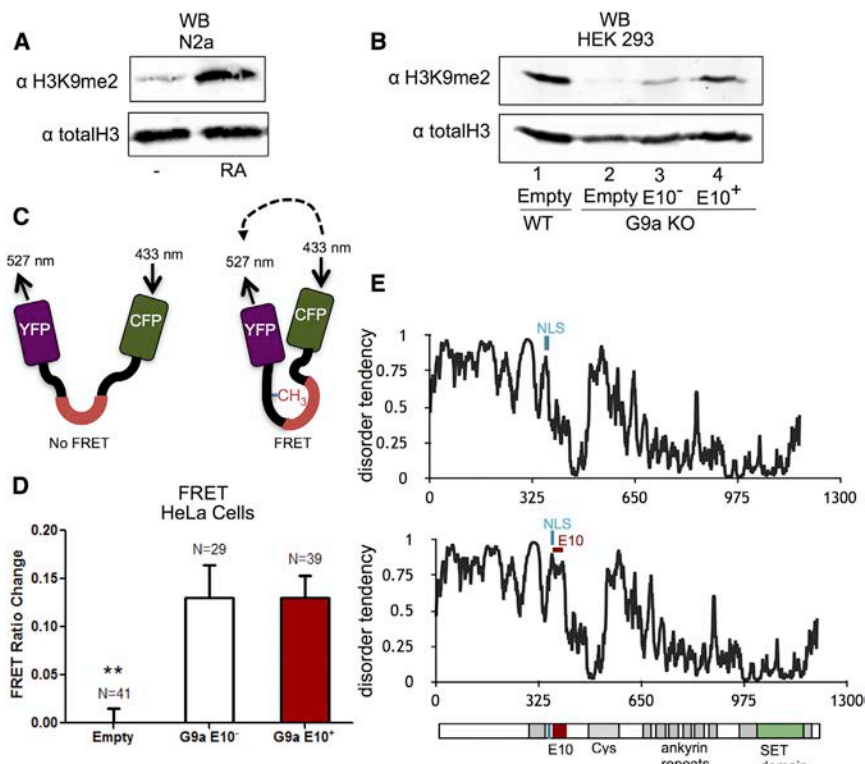


Figure 4. E10 Inclusion Stimulates H3K9me2 without Affecting G9a Catalytic Activity

(A) Following differentiation with 1 μM RA for 3 days, N2a cells were harvested and western blot performed with anti-H3K9me2 and anti-total H3 antibodies.

(B) G9a CRISPR-ablated HEK293 cells were transfected with expression plasmids encoding mouse E10⁻, E10⁺ G9a full-length cDNAs or the corresponding empty vector. 48 hr after transfection, cells were harvested and western blot assay was performed as in (A).

(C) Schematic diagram of the methyltransferase activity reporter (Lin et al., 2004).

(D) HeLa cells were co-transfected with expression plasmids encoding mouse E10⁻ or E10⁺ G9a isoforms and the methyltransferase activity reporter. Methylation of the reporter protein was detected by FRET as described in Experimental Procedures. FRET data were obtained only from nuclear compartments of cells. Bars represent means ± SE. Nonparametric Wilcoxon rank-sum test was used (**p < 0.001).

(E) Predicted disorder of the polypeptides encoded by the G9a splicing variants. The energy of each residue of E10⁻ (top) and E10⁺ (bottom) G9a isoforms was calculated by IUPred to assign their order/disorder status, as described in Experimental Procedures.

histone deacetylase inhibitor trichostatin A (TSA) have been shown to alter DNA methylation and histone acetylation, resulting in reduced H3K9me2 levels (Coombes et al., 2003; Fahrner et al., 2002; Nguyen et al., 2002). In our system, both 5aC and TSA also prevent E10 increased inclusion during neuron differentiation, further supporting a role for histone marks in the regulation of G9a E10 splicing (Figures S4B and S4C). Of note, bisulfite sequencing analysis of a CpG island located in G9a intron 9 shows no changes in 5-methylcytosine upon differentiation of N2a cells, indicating that the effect of 5aC on E10 inclusion is not due to inhibition of DNA methylation (Figure S4D). Altogether, these observations suggest that chromatin structure plays a fundamental role in the regulation of G9a alternative splicing.

To further examine the role of G9a in the regulation of alternative splicing of its own pre-mRNA, we obtained a G9a splicing reporter minigene containing exons 9–11 and their corresponding introns (Figure S5A) which, when transfected into N2a cells, shows the same regulation as the endogenous gene during neuron differentiation (Figure S5B). PCR primers used to amplify the minigene transcripts were designed so as to avoid detecting the G9a expressed isoforms (Figure 7B, right three lanes). Cotransfection of the G9a splicing reporter with the expression constructs encoding the G9a isoforms shows that the E10⁺ is more powerful than the E10⁻ isoform in stimulating E10 inclusion in HeLa cells (Figure 7B, left three lanes). This effect is significantly reduced when the E10⁺ catalytically dead mutant is overexpressed (Figure 7C). The inhibitory effect is even stronger when expressing another E10⁺ mutant that also has its interaction with GLP impaired (Tachibana et al., 2008) (Figure 7D) and is also observed upon G9a activity inhibition by treatment with BIX (Figure 7E).

Taken together, our results suggest that G9a affects its own alternative splicing either in a direct or indirect manner. Moreover, this regulation requires interaction with GLP and G9a methyltransferase activity. As G9a E10⁺ isoform is more potent at promoting E10 inclusion and is required for efficient neuron differentiation, our results are consistent with a positive loop in which neuron differentiation favors the synthesis of the E10⁺ isoform that, in turn, promotes more inclusion of E10 and favors the nuclear localization of the protein.

DISCUSSION

Intragenic histone modifications control alternative splicing through either the modulation of RNAPII elongation rates or the recruitment of adaptors and splicing factors to the pre-mRNA that is being synthesized. The existence of such mechanisms, which are not mutually exclusive, imposes the study of the regulation of the enzymes in charge of writing the specific histone marks that regulate alternative splicing. We have chosen G9a because in addition to its fundamental role in the regulation of gene expression programs triggered by cellular differentiation, the silencing mark H3K9me2 has been shown to contribute to several alternative splicing decisions (Saint-André et al., 2011; Salton et al., 2014; Schor et al., 2013).

Papasaikas and colleagues have recently reported a functional interaction alternative splicing network where most of the nodes are occupied by splicing regulators with a few cases of chromatin factors (Papasaikas et al., 2015). Interestingly, and despite the fact that the majority of the chromatin factors appear peripherally in the network, G9a and SUV39H1 are centrally

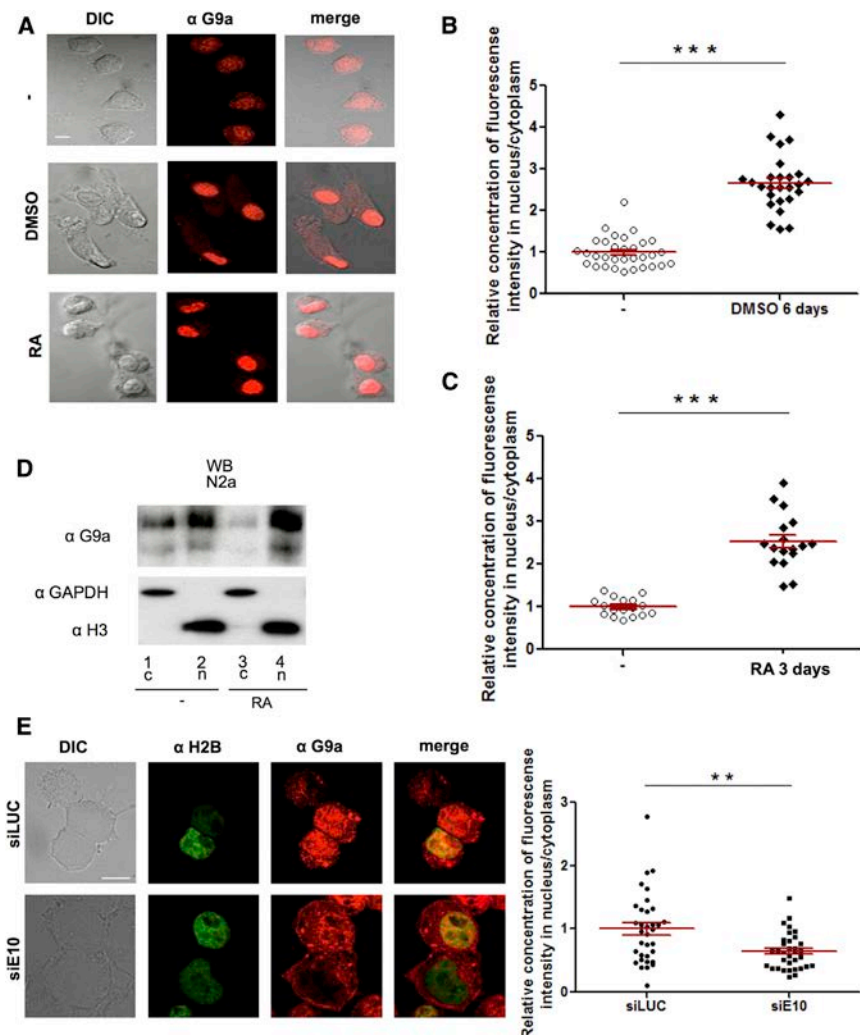


Figure 5. Neuronal Differentiation Triggers a Nuclear Accumulation of G9a Protein

N2a cells were differentiated with 2% (v/v) DMSO or 1 μ M RA for 6 or 3 days, respectively.

(A) Cells were then fixed and G9a protein localization was assessed by indirect immunofluorescence.

(B and C) Plots show relative concentration of fluorescence intensity of G9a in the nuclear and cytoplasmic compartments for N2a cells differentiated with DMSO (B) or RA (C).

(D) After differentiation with 1 μ M RA for 3 days, N2a cells were harvested and nuclear and cytoplasmic fractions obtained and treated for denaturing SDS-PAGE, followed by western blot with anti-H3, anti-GAPDH, and anti-G9a antibodies.

(E) Undifferentiated N2a cells were transfected with siE10 or siLUC as a control and fixed for immunofluorescence as in (A). The plot on the right shows relative concentration of fluorescence intensity of G9a in the nuclear and cytoplasmic compartments 48 hr after transfection.

Scale bars represent 10 μ m. Statistical analysis corresponds to Student's t test (** p < 0.001 and *** p < 0.0001). See also Figure S2.

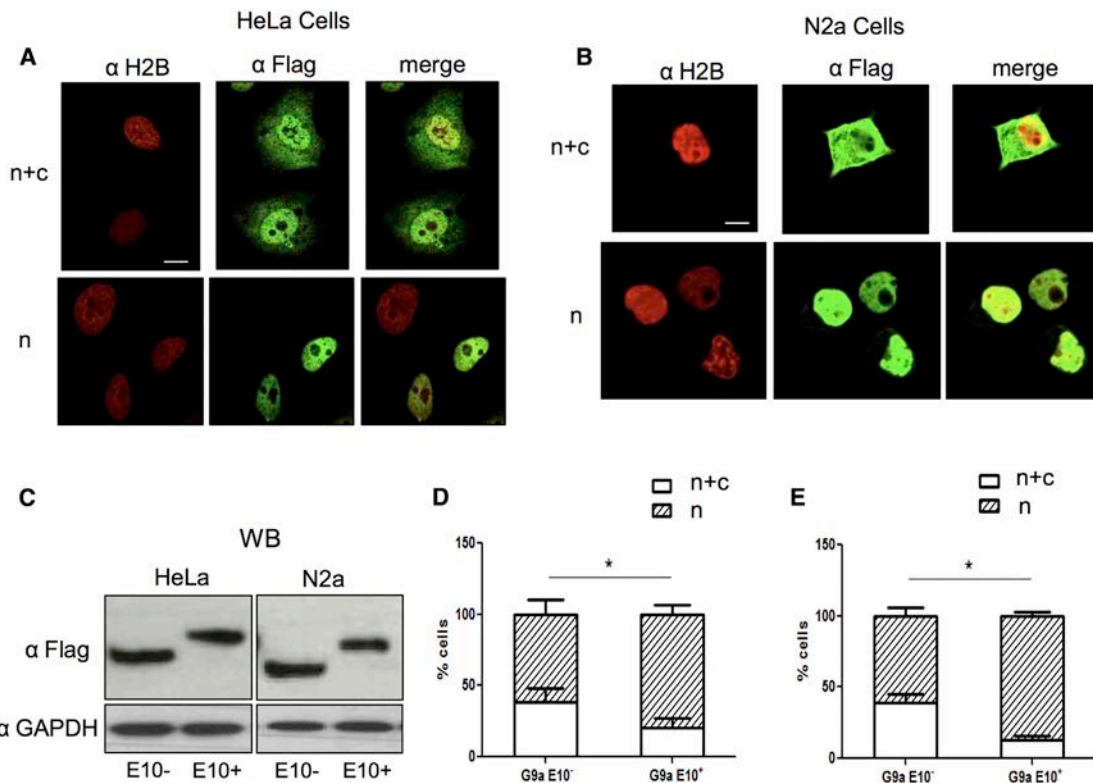
localized with strong connections to core spliceosomal factors—mainly U5 components—suggesting mechanistic cross-talks between their function and the regulation of alternative splicing (Figure S6).

We report here that G9a is required for neuron differentiation of N2a cells in culture, consistent with higher H3K9me2 global levels in differentiated cells. This observation is not surprising, as G9a has been shown to affect a variety of differentiation pathways (Lehnertz et al., 2010; Ling et al., 2012; Wada et al., 2015), in addition to its implications in the development of neural tissues (Maze et al., 2014; Schaefer et al., 2009; Subbanna et al., 2013). Moreover, our results show that G9a regulation takes place at the level of alternative splicing by a positive feedback loop. We observed that inclusion of G9a E10 increases during neuron differentiation (Figure 2) and that the E10⁺ G9a isoform favors the inclusion of E10 in the mature mRNA and is required for efficient neuron differentiation (Figures 3B and 3C). It is likely that this positive loop is part of the differentiation program of different cell types, since the effect on E10 inclusion is not restricted to neuron development (Figure 2F).

Multiple independent lines of evidence demonstrate that G9a's histone-methylating activity regulates alternative splicing of its own pre-mRNA: differentiation-dependent E10 inclusion is abrogated by the inhibitor of H3K9 dimethylation BIX 01894 (Figure 7A), by drugs that indirectly promote H3K9 demethylation like 5aC and TSA (Figures S4B and S4C), and by mutating G9a's catalytic site (Figures 7C and 7D). All these data are consistent with higher levels of H3K9me2 deployed on the G9a gene

upon neuron differentiation (Figure S4A). It is important to point out that the increase in H3K9me2 on the G9a gene was relativized to total H3, indicating that differentiation does not merely increase nucleosome density on the G9a gene but changes the quality of its histone marks. The deployment of this silencing mark does not seem to be specific for the G9a gene, as it has been also observed in the NCAM gene (Schor et al., 2013) as well as in the fibronectin gene (Figure S7) upon neuron differentiation. We do not rule out the possibility of an indirect mechanism of G9a regulating its own alternative splicing.

Regarding the mechanism by which G9a methylating activity regulates its own alternative splicing, one obvious inference would be a positive feedback loop in which inclusion of E10 would upregulate G9a enzymatic activity. However, we demonstrate here that E10 inclusion does not affect the enzyme activity *in vivo* (Figure 4D). Instead, the intrinsically unstructured nature of the E10 peptide, characteristic of most protein segments encoded by alternatively spliced exons (Buljan et al., 2013), might contribute to a major exposure of a neighboring NLS (Figure 4E), suggesting that E10 inclusion promotes G9a nuclear localization. This prediction is

**Figure 6. Presence of Exon 10 Favors G9a Nuclear Localization**

(A and B) HeLa (A) or N2a cells (B) were transfected with expression plasmids encoding mouse Flag-tagged E10⁻ or E10⁺ G9a full-length cDNAs (corresponding to the short isoforms according to the promoter, including the distal first exon). 48 hr after transfection, cells were fixed and Flag-tagged G9a protein localization was assessed by indirect immunofluorescence. The nuclear histone 2B protein was used as a control. Cells with both nuclear and cytoplasmic (n+c) or nuclear only (n) G9a localization are shown.

(C) Expression levels of the E10⁻ or E10⁺ G9a isoforms were determined by western blot in transfected HeLa (left) or N2a cells (right).

(D and E) Bars show the percentage of HeLa (D) and N2a cells (E) with n+c or n G9a signal (n = between 31 and 208 cells). Scale bars represent 10 μ m. Statistical analysis corresponds to Fisher exact test (*p < 0.05).

confirmed indirectly in Figure 5 and directly by evaluating the localization of flag-tagged G9a, containing or lacking E10, transiently expressed in HeLa and N2a cells (Figure 6). Results in Figure 6 can be explained if one takes into account that the overexpressed recombinant G9a polypeptide does not enter the nucleus alone but in multisubunit complexes containing GLP and endogenous G9a polypeptides that may or may not contain E10. This idea is reinforced by our evidence that a G9a mutant in which interaction with GLP is abolished is more defective in promoting E10 inclusion (Figure 7D). In this context, it is predictable that the overexpression of G9a E10⁺ will change the balance in the percentage of cells displaying the n+c and the n patterns toward the latter. The observation that G9a is present not only in the nucleus but also in the cytoplasm during some conditions may explain some of the G9a reported interactions with non-histone targets. Indeed, over 500 predicted targets of G9a and GLP have been identified, more than 50% of which do not localize in the nucleus (Islam et al., 2013).

A relevant report was published aimed at studying the roles of alternative splicing both of G9a and the heterochromatin histone methyltransferase SUV39H2 (Mauger et al., 2015). The authors found that inclusion of SUV39H2 alternative exon 3 is key for the subnuclear localization and catalytic activity of this enzyme.

Regarding the inclusion of E10 in G9a, similarly to our results obtained *in vivo* with the methylation FRET reporter, the authors did not report changes in G9a activity measured *in vitro*. However, unlike our findings, the authors did not see differences in the subcellular localization of the E10⁺ and E10⁻ isoforms, leading them to conclude that since the levels of E10 inclusion vary greatly in different cell types, alternative splicing of E10 must be controlling G9a properties other than its methyltransferase activity or localization. The contrasting observations may rely on different models of study.

Our results reveal a positive feedback loop in which E10 inclusion increases during neuronal differentiation and favors G9a nuclear localization, subsequently upregulating E10 inclusion (Figure 7F). We propose that G9a triggers a positive loop that helps maintaining the genetic expression program and, thus, reinforces the cellular commitment to neuron differentiation.

EXPERIMENTAL PROCEDURES

Cell Culture and Treatments

N2a cells were grown in DMEM, with high glucose and pyruvate (Invitrogen), supplemented with 10% fetal bovine serum (FBS). For differentiation with

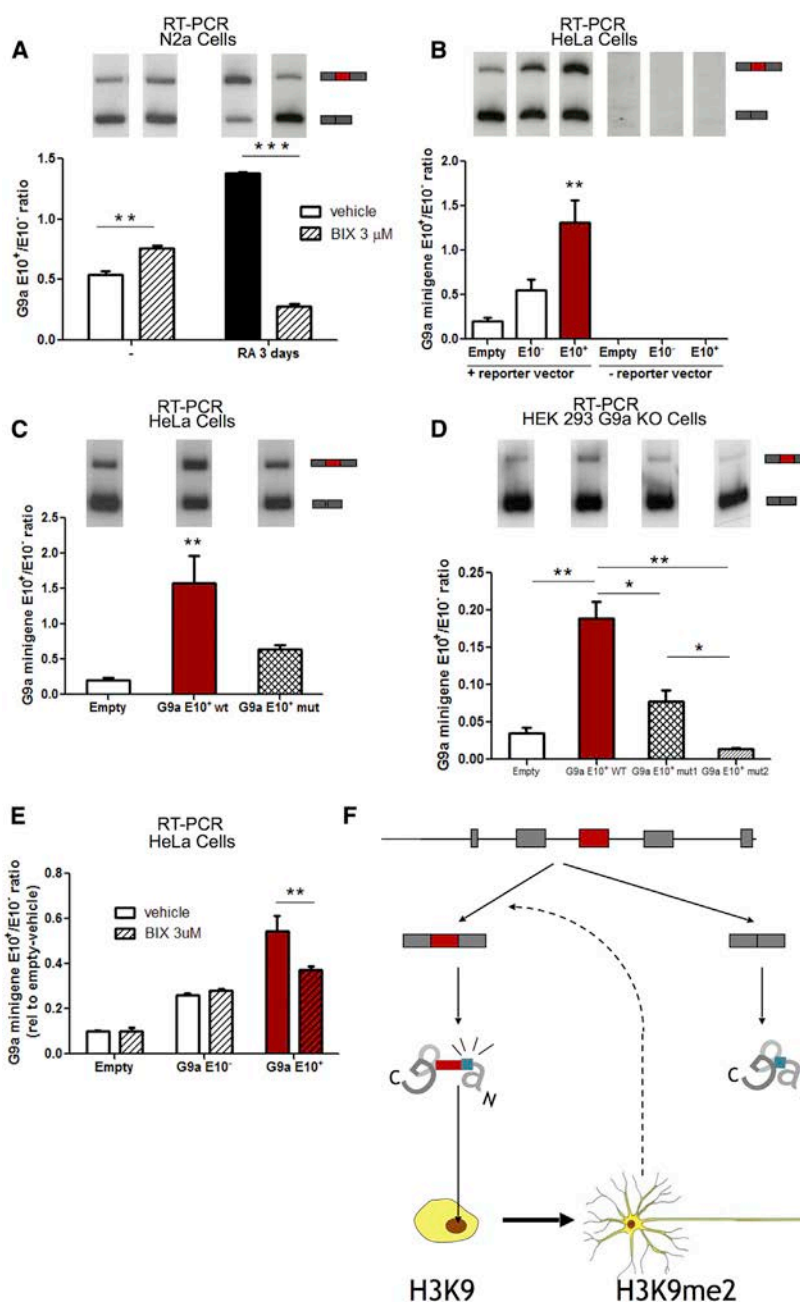


Figure 7. G9a Methyltransferase Activity Is Involved in the Regulation of Its Own Alternative Splicing

(A) N2a cells were differentiated with 1 μ M RA for 3 days and treated with vehicle or 3 μ M BIX. Cells were then harvested, RNA was extracted, and alternative splicing of G9a was assessed as described in Figure 2. See also Figure S3.

(B-D) Cells were co-transfected with a reporter minigene for E10 alternative splicing together with expression plasmids encoding mouse E10⁻, E10⁺ G9a full-length cDNAs, or the corresponding empty vectors. In (C), a catalytic mutant version of the E10⁺ G9a isoform was tested in HeLa cells, and in (D), two catalytic mutant versions of the E10⁺ G9a isoform were tested in G9a CRISPR-ablated HEK293 cells. RT-PCR gels are shown at the top and the corresponding quantification at the bottom.

(E) The effect of 3 μ M BIX was assayed, and results are shown normalized to values with empty vector for vehicle or BIX treatment. Cells were harvested 48 hr after transfection, and alternative splicing of G9a was assessed by radioactive RT-PCR using minigene-specific primers.

(F) Model for the roles of G9a alternative splicing. In undifferentiated cells, the prevalence of E10 exclusion isoform of G9a correlates with low nuclear localization signal of the protein. Being required for neuron differentiation, G9a preferentially localizes to the nucleus upon differentiation, correlating with an alternative splicing pattern of the G9a gene that favors the E10⁺ G9a form. This change is accompanied by increased levels of H3K9 methylation of the G9a gene and requires G9a methyltransferase activity, suggesting a positive feedback loop in which G9a regulates its own alternative splicing.

All experiments were performed in triplicate, and means and SE of representative experiments are shown. Statistical analysis corresponds to one-way or two-way ANOVA, Bonferroni post hoc test (* $p < 0.05$, ** $p < 0.001$, and *** $p < 0.0001$). See also Figures S4 and S5.

DMSO, 200,000 cells were plated and the next day were washed once with PBS and incubated for 4 to 8 days in the same medium but with 0.2% serum and 2% DMSO. For differentiation with RA, 200,000 cells were plated and the next day washed once with PBS and incubated for 1–3 days in the same medium without pyruvate and with 1 μ M RA.

P19 cells were grown in α -minimum essential medium (Invitrogen) supplemented with 7.5% newborn calf serum and 2.5% fetal calf serum. For differentiation to neural cells, P19 supplemented with 10% FBS were subjected to treatment with RA to induce the cells to form embryoid bodies for 4 days. The disaggregated cells were then plated on polylysine and grown in neurobasal medium supplemented with B27 for 3–4 more days.

For BIX 01294 (Sigma) treatment, drug or vehicle was added to differentiated cells with RA or to undifferentiated cells plated at low confluence and

left for 2–3 days. In order to address the role of G9a during neuron differentiation, treatment with BIX or siG9a was performed prior to the differentiation process. 6 hr after transfection/treatment, neuron differentiation was induced with RA.

For 5-azacytidine (Sigma) treatment, drug or vehicle was added to differentiated cells with

DMSO at day 5–6 or to undifferentiated cells plated at low confluence and left for 3 days. For trichostatin A (Sigma) treatments, the drug or vehicle was left overnight (16 hr) at day 6–7 in differentiated cells with DMSO or undifferentiated cells.

For quantification of neuron differentiation, neurite morphology of N2a cells was monitored. Cells with a total neurite length >2-fold higher than the soma diameter were considered to be differentiated as previously described (Chen et al., 2012).

Functionally normal mammary epithelial cells (EpH4) were routinely grown in DMEM:F-12 (Invitrogen) supplemented with 2% FBS (GIBCO), insulin (5 μ g/ml, Sigma), and gentamicin (50 μ g/ml; Invitrogen). At the onset of the experiments, 1 \times 105 cells were plated either on plastic 35-mm tissue culture wells or on Matrigel pre-coated ones in DMEM-F12 medium supplemented with insulin

and the lactogenic hormones hydrocortisone (1 µg/ml; Sigma) and prolactin (3 µg/ml; Sigma), as well as 2% FBS. After 24 hr, the medium was replaced with serum-free DMEM:F12 plus insulin and lactogenic hormones, and the cells were maintained under these conditions for 6 days, with medium replacement every 48 hr. Upon this treatment, cells undergo a morphogenic process that leads to the formation of polarized three-dimensional structures that turn on milk protein gene expression or directly on tissue culture plastic, where this morphological and functional differentiation does not occur.

RNA Extraction and RT-PCR

Total RNA was extracted using TRI Reagent (Molecular Research Center) according to the manufacturer's protocol. Reverse transcription using M-MLV reverse transcriptase (Invitrogen) and oligo-dT primer was performed according to the provider's instructions. Analysis of G9a E10 splicing was performed using semiquantitative radioactive PCR. All PCR conditions and primer sequences are available upon request.

siRNA Transfections

For total G9a knockdown, the pool of siRNA oligonucleotides used was siGENOME Mouse Ehmt2 (catalog number M-053728-00-0005; Dharmacon). For G9a E10⁺ knockdown, a specific siRNA (Invitrogen) was designed to target 25 nt from the E10 sequence (sense, 5'-CCCAGUGAGUGGAGCUGCC CAGCGA-3'; antisense: 5'-UCGCUGGGCAGCUCCACUCUGGG-3'). 5 µl 20-µM siRNA was transfected into cells using Lipofectamine 2000 (Life Technologies) transfection reagent in accordance with the supplier's recommendations.

Plasmids

Mouse Flag-G9a E10⁺, mouse Flag-G9a E10⁻, human G9a E10⁺ catalytic mutants 1 and 2 were cloned in the pcDNA3 backbone. Mouse pCAG G9a full-length (G9a E10⁺ wt) and catalytic mutant (G9a E10⁺ mut) were kindly donated by Dr. Slimane and Dr. Shinkai. For transfection assays, 1 µg plasmid was transfected into each well of a 6-wells culture plate using Lipofectamine 2000 reagent (Life Technologies) according to the manufacturer's recommendations.

Antibodies

G9a antibody (#3306) and Flag antibody (#2368) from Cell Signaling were used in western blot assays, immunofluorescence, and FRET. G9a human antibody from Genetex (GTX63007) and G9a mouse antibody from Sigma (SAB2700645) were used in immunofluorescence experiments. H3K9me2 (#07-441) and H3total (#07-690) from Millipore were used in western blot assays.

Immunofluorescence Microscopy

Cells were grown on coverslips and fixed with 4% paraformaldehyde for 15 min at room temperature. Cells were then permeabilized with 0.1% Triton X-100 for 5 min at room temperature followed by 30 min of blocking with 1% non-immune normal goat serum (catalog number 50-197Z; Invitrogen). Coverslips were subsequently incubated for 1 hr in primary antibody and 1 hr in secondary antibody diluted in blocking solution. Coverslips were mounted with PBS:glycerol 1:1 (v/v). Images were acquired with an Olympus FV1000 inverted confocal microscope using a 60× oil-immersion objective and processed using FluorView Viewer software (Olympus).

FRET Imaging and Analysis

HeLa cells were co-transfected with expression plasmids encoding mouse E10⁻ or E10⁺ G9a isoforms and a methyltransferase activity reporter (Lin et al., 2004) based on the CFP/YFP FRET pair. Cells co-transfected with the FRET reporter and an empty vector were used as control for estimating a basal FRET. The expression of the E10⁻ or E10⁺ plasmids was evaluated by immunofluorescence using indirect immunofluorescence with an anti-Flag as a primary antibody. Images were collected on an Olympus FV1000 inverted confocal microscope, using a 100× numerical aperture (NA) 1.4 oil-immersion objective lens. For each data acquisition, five images were collected using the FluorView software virtual channel function: a simultaneous acquisition of a CFP image (440-nm laser, 480- to 495-nm emission filter) and a FRET image (440-nm laser, 535- to 565-nm emission filter) at the virtual channel at phase 1, and a sequential acquisition of a YFP image (515-nm laser, 550- and 610-nm emission filter) and a RED image (635-nm laser, 655- to 755-nm emission filter)

together with a transmitted light image were collected at phase 2. Background subtraction from all channels was performed before quantitative manipulations of the images. Nuclei segmentation was performed by global thresholding of the RED channel. The FRET ratio was calculated pixel by pixel as $R_{FRET} = FRET/CFP$ and evaluated for each cell by quantifying mean and SD from pixels inside nuclei masks.

At each condition, between 29 and 41 cells were analyzed, and the average FRET ratio was calculated for cells expressing the inclusion or exclusion isoform and for control cells. FRET ratio change was defined as the relative change with respect to the control cell FRET ratio (FRET ratio change = $(R_{ISOFORM\ FRET} - R_{CONTROL\ FRET})/R_{CONTROL\ FRET}$). The nonparametric Wilcoxon rank-sum test was employed to assess whether the different populations were statistically different.

Disorder Prediction

G9a disordered regions were predicted with the web-based program IUPred (<http://iupred.enzim.hu>), using the long disorder prediction type. IUPred uses a statistical potential to calculate the energy of each residue in a given sequence and to assign their order/disorder status (1, 2). This potential was derived from a dataset of protein with known structures, and the calculated energy is averaged over a sliding window of 21 residues.

Animals

C57BL/6J mice from the strain of the Bioterio Central, Facultad de Ciencias Exactas y Naturales (University of Buenos Aires) were used for all experiments. Animals were kept in a 12:12 hr light:dark cycle with lights on at 6 am, and food and water were administered ad libitum. Experiments were performed in accordance with local regulations and the National Institutes of Health (NIH) *Guide of the Care and Use of Laboratory Animals* (NIH publication 80-23/96) and were previously approved by the Ethical Committee (CICUAL) of the Facultad de Ciencias Exactas y Naturales, University of Buenos Aires. All efforts were made to minimize animal suffering and to reduce the number of animals used.

Mice were previously anesthetized with Avertin 2% and then sacrificed by cervical dislocation at indicated postnatal days (PNDs): PND 1, PND 7, and PND 120. Whole brain was extracted, rapidly frozen in liquid N₂, and stored at -80°C. Isolation of RNA was carried out using TRI-Reagent (Molecular Research Center), and preparation of cDNA was performed using M-MLV Reverse Transcriptase (Promega). Alternative splicing of G9a was determined through PCR as previously described.

Statistical Analysis

GraphPad Prism 5 was used for statistical analysis. One-way or two-way ANOVA tests were followed by Bonferroni's corrected multiple comparisons between pairs of conditions, or TTEST comparisons were used with just two pair of conditions. Unless otherwise indicated in the figure legends, we analyzed three biological replicates for each data point in all graphs, and the level of significance was as follows: *p < 0.05, **p < 0.01, and ***p < 0.001.

SUPPLEMENTAL INFORMATION

Supplemental Information includes Supplemental Experimental Procedures and seven figures and can be found with this article online at <http://dx.doi.org/10.1016/j.celrep.2016.02.063>.

AUTHOR CONTRIBUTIONS

A.F. and A.R.K. designed and A.F. performed most of the experiments. L.E.G., A.Q., B.G.B., L.S., C.v.B., I.E.S., L.I.P., J.J.C., and A.S. performed some of the experiments and participated with helpful discussions and ideas. J.H.E.S. and M.R. provided reagents. A.F., L.E.G., and A.R.K. wrote the manuscript. A.R.K. supervised the whole work.

ACKNOWLEDGMENTS

We thank Kristen Lynch and Nicole M. Martinez for providing the G9a mini-gene, Yoichi Shinkai and Slimane Ait-Si-Ali for providing G9a expression

vectors, Valeria Buggiano for technical support, and Alejandro Colman Lerner as well as members of the Kornblith lab for their support and useful discussions. The research was supported by grants to A.R.K. and A.S. from the Agencia Nacional de Promoción de Ciencia y Tecnología of Argentina, the Universidad de Buenos Aires and the European Alternative Splicing Network (EURASNET). A.R.K., A.S., L.E.G., L.S., I.E.S., M.R., L.I.P., and J.J.C. are career investigators; C.v.B. is recipient of a postdoctoral fellowship; and A.F., B.G.B., and J.H.E.S. are recipients of doctoral fellowships, all from the Consejo Nacional de Investigaciones Científicas y Técnicas of Argentina (CONICET). A.R.K. is a Senior International Research Scholar of the Howard Hughes Medical Institute.

Received: December 7, 2015

Revised: January 25, 2016

Accepted: February 12, 2016

Published: March 17, 2016

REFERENCES

- Adami, G., and Babiss, L.E. (1991). DNA template effect on RNA splicing: two copies of the same gene in the same nucleus are processed differently. *EMBO J.* **10**, 3457–3465.
- Alló, M., Buggiano, V., Fededa, J.P., Petrillo, E., Schor, I., de la Mata, M., Agirre, E., Plass, M., Eyras, E., Elela, S.A., et al. (2009). Control of alternative splicing through siRNA-mediated transcriptional gene silencing. *Nat. Struct. Mol. Biol.* **16**, 717–724.
- Alló, M., Agirre, E., Bessonov, S., Bertucci, P., Gómez Acuña, L., Buggiano, V., Bellora, N., Singh, B., Petrillo, E., Blaustein, M., et al. (2014). Argonaute-1 binds transcriptional enhancers and controls constitutive and alternative splicing in human cells. *Proc. Natl. Acad. Sci. USA* **111**, 15622–15629.
- Ameyar-Zazoua, M., Rachez, C., Souidi, M., Robin, P., Fritsch, L., Young, R., Morozova, N., Fenouil, R., Descotes, N., Andrau, J.C., et al. (2012). Argonaute proteins couple chromatin silencing to alternative splicing. *Nat. Struct. Mol. Biol.* **19**, 998–1004.
- Bannister, A.J., and Kouzarides, T. (2011). Regulation of chromatin by histone modifications. *Cell Res.* **21**, 381–395.
- Barbosa-Morais, N.L., Irimia, M., Pan, Q., Xiong, H.Y., Gueroussov, S., Lee, L.J., Slobodeniuc, V., Kutter, C., Watt, S., Colak, R., et al. (2012). The evolutionary landscape of alternative splicing in vertebrate species. *Science* **338**, 1587–1593.
- Batsché, E., Yaniv, M., and Muchardt, C. (2006). The human SWI/SNF subunit Brm is a regulator of alternative splicing. *Nat. Struct. Mol. Biol.* **13**, 22–29.
- Bentley, D.L. (2005). Rules of engagement: co-transcriptional recruitment of pre-mRNA processing factors. *Curr. Opin. Cell Biol.* **17**, 251–256.
- Brown, S.E., Campbell, R.D., and Sanderson, C.M. (2001). Novel NG36/G9a gene products encoded within the human and mouse MHC class III regions. *Mamm. Genome* **12**, 916–924.
- Buljan, M., Chalancon, G., Dunker, A.K., Bateman, A., Balaji, S., Fuxreiter, M., and Babu, M.M. (2013). Alternative splicing of intrinsically disordered regions and rewiring of protein interactions. *Curr. Opin. Struct. Biol.* **23**, 443–450.
- Cáceres, J.F., and Kornblith, A.R. (2002). Alternative splicing: multiple control mechanisms and involvement in human disease. *Trends Genet.* **18**, 186–193.
- Chang, Y., Zhang, X., Horton, J.R., Upadhyay, A.K., Spannhoff, A., Liu, J., Snyder, J.P., Bedford, M.T., and Cheng, X. (2009). Structural basis for G9a-like protein lysine methyltransferase inhibition by BIX-01294. *Nat. Struct. Mol. Biol.* **16**, 312–317.
- Chen, H.H., Yu, H.I., Chiang, W.C., Lin, Y.D., Shia, B.C., and Tarn, W.Y. (2012). hnRNP Q regulates Cdc42-mediated neuronal morphogenesis. *Mol. Cell. Biol.* **32**, 2224–2238.
- Chin, H.G., Estève, P.O., Pradhan, M., Benner, J., Patnaik, D., Carey, M.F., and Pradhan, S. (2007). Automethylation of G9a and its implication in wider substrate specificity and HP1 binding. *Nucleic Acids Res.* **35**, 7313–7323.
- Collins, R.E., Northrop, J.P., Horton, J.R., Lee, D.Y., Zhang, X., Stallcup, M.R., and Cheng, X. (2008). The ankyrin repeats of G9a and GLP histone methyltransferases are mono- and dimethyllysine binding modules. *Nat. Struct. Mol. Biol.* **15**, 245–250.
- Coombes, M.M., Briggs, K.L., Bone, J.R., Clayman, G.L., El-Naggar, A.K., and Dent, S.Y. (2003). Resetting the histone code at CDKN2A in HNSCC by inhibition of DNA methylation. *Oncogene* **22**, 8902–8911.
- Dosztányi, Z., Csizmok, V., Tompa, P., and Simon, I. (2005). IUPred: web server for the prediction of intrinsically unstructured regions of proteins based on estimated energy content. *Bioinformatics* **21**, 3433–3434.
- Ellis, J.D., Barrios-Rodiles, M., Colak, R., Irimia, M., Kim, T., Calarco, J.A., Wang, X., Pan, Q., O'Hanlon, D., Kim, P.M., et al. (2012). Tissue-specific alternative splicing remodels protein-protein interaction networks. *Mol. Cell* **46**, 884–892.
- Fahrner, J.A., Eguchi, S., Herman, J.G., and Baylin, S.B. (2002). Dependence of histone modifications and gene expression on DNA hypermethylation in cancer. *Cancer Res.* **62**, 7213–7218.
- Faustino, N.A., and Cooper, T.A. (2003). Pre-mRNA splicing and human disease. *Genes Dev.* **17**, 419–437.
- Gonzalez, I., Munita, R., Aguirre, E., Dittmer, T.A., Gysling, K., Misteli, T., and Luco, R.F. (2015). A lncRNA regulates alternative splicing via establishment of a splicing-specific chromatin signature. *Nat. Struct. Mol. Biol.* **22**, 370–376.
- Huang, J., Dorsey, J., Chuikov, S., Pérez-Burgos, L., Zhang, X., Jenuwein, T., Reinberg, D., and Berger, S.L. (2010). G9a and GLP methylate lysine 373 in the tumor suppressor p53. *J. Biol. Chem.* **285**, 9636–9641.
- Islam, K., Chen, Y., Wu, H., Bothwell, I.R., Blum, G.J., Zeng, H., Dong, A., Zheng, W., Min, J., Deng, H., and Luo, M. (2013). Defining efficient enzyme-cofactor pairs for bioorthogonal profiling of protein methylation. *Proc. Natl. Acad. Sci. USA* **110**, 16778–16783.
- Jenuwein, T., and Allis, C.D. (2001). Translating the histone code. *Science* **293**, 1074–1080.
- Kadener, S., Cramer, P., Nogués, G., Cazalla, D., de la Mata, M., Fededa, J.P., Werbajh, S.E., Srebrow, A., and Kornblith, A.R. (2001). Antagonistic effects of T-Ag and VP16 reveal a role for RNA pol II elongation on alternative splicing. *EMBO J.* **20**, 5759–5768.
- Kelemen, O., Convertini, P., Zhang, Z., Wen, Y., Shen, M., Falaleeva, M., and Stamm, S. (2013). Function of alternative splicing. *Gene* **514**, 1–30.
- Kolasinska-Zwierz, P., Down, T., Latorre, I., Liu, T., Liu, X.S., and Ahringer, J. (2009). Differential chromatin marking of introns and expressed exons by H3K36me3. *Nat. Genet.* **41**, 376–381.
- Kornblith, A.R., Schor, I.E., Alló, M., Dujardin, G., Petrillo, E., and Muñoz, M.J. (2013). Alternative splicing: a pivotal step between eukaryotic transcription and translation. *Nat. Rev. Mol. Cell Biol.* **14**, 153–165.
- Kramer, J.M. (2015). Regulation of cell differentiation and function by the euchromatin histone methyltransferases G9a and GLP. *Biochem. Cell Biol.* **94**, 26–32.
- Kramer, J.M., Kochinke, K., Oortveld, M.A., Marks, H., Kramer, D., de Jong, E.K., Asztalos, Z., Westwood, J.T., Stunnenberg, H.G., Sokolowski, M.B., et al. (2011). Epigenetic regulation of learning and memory by Drosophila EHMT/G9a. *PLoS Biol.* **9**, e1000569.
- Kubicek, S., O'Sullivan, R.J., August, E.M., Hickey, E.R., Zhang, Q., Teodoro, M.L., Rea, S., Mechta, K., Kowalski, J.A., Homon, C.A., et al. (2007). Reversal of H3K9me2 by a small-molecule inhibitor for the G9a histone methyltransferase. *Mol. Cell* **25**, 473–481.
- Lehnertz, B., Northrop, J.P., Antignano, F., Burrows, K., Hadidi, S., Mullaly, S.C., Rossi, F.M., and Zaph, C. (2010). Activating and inhibitory functions for the histone lysine methyltransferase G9a in T helper cell differentiation and function. *J. Exp. Med.* **207**, 915–922.
- Lin, C.W., Jao, C.Y., and Ting, A.Y. (2004). Genetically encoded fluorescent reporters of histone methylation in living cells. *J. Am. Chem. Soc.* **126**, 5982–5983.
- Ling, B.M., Gopinadhan, S., Kok, W.K., Shankar, S.R., Gopal, P., Bharathy, N., Wang, Y., and Taneja, R. (2012). G9a mediates Sharp-1-dependent inhibition of skeletal muscle differentiation. *Mol. Biol. Cell* **23**, 4778–4785.

- Liu, H., He, L., and Tang, L. (2012). Alternative splicing regulation and cell lineage differentiation. *Curr. Stem Cell Res. Ther.* 7, 400–406.
- Liu, N., Zhang, Z., Wu, H., Jiang, Y., Meng, L., Xiong, J., Zhao, Z., Zhou, X., Li, J., Li, H., et al. (2015). Recognition of H3K9 methylation by GLP is required for efficient establishment of H3K9 methylation, rapid target gene repression, and mouse viability. *Genes Dev.* 29, 379–393.
- Luco, R.F., Pan, Q., Tominaga, K., Blencowe, B.J., Pereira-Smith, O.M., and Misteli, T. (2010). Regulation of alternative splicing by histone modifications. *Science* 327, 996–1000.
- Martinez, N.M., Pan, Q., Cole, B.S., Yarosh, C.A., Babcock, G.A., Heyd, F., Zhu, W., Ajith, S., Blencowe, B.J., and Lynch, K.W. (2012). Alternative splicing networks regulated by signaling in human T cells. *RNA* 18, 1029–1040.
- Mauger, O., Klinck, R., Chabot, B., Muchardt, C., Allemand, E., and Batsché, E. (2015). Alternative splicing regulates the expression of G9A and SUV39H2 methyltransferases, and dramatically changes SUV39H2 functions. *Nucleic Acids Res.* 43, 1869–1882.
- Maze, I., Chaudhury, D., Dietz, D.M., Von Schimmelmann, M., Kennedy, P.J., Lobo, M.K., Sillivan, S.E., Miller, M.L., Bagot, R.C., Sun, H., et al. (2014). G9a influences neuronal subtype specification in striatum. *Nat. Neurosci.* 17, 533–539.
- Naftelberg, S., Schor, I.E., Ast, G., and Kornblhtt, A.R. (2015). Regulation of alternative splicing through coupling with transcription and chromatin structure. *Annu. Rev. Biochem.* 84, 165–198.
- Neugebauer, K.M. (2002). On the importance of being co-transcriptional. *J. Cell Sci.* 115, 3865–3871.
- Nguyen, C.T., Weisenberger, D.J., Velicescu, M., Gonzales, F.A., Lin, J.C., Liang, G., and Jones, P.A. (2002). Histone H3-lysine 9 methylation is associated with aberrant gene silencing in cancer cells and is rapidly reversed by 5-aza-2'-deoxycytidine. *Cancer Res.* 62, 6456–6461.
- Ohno, H., Shinoda, K., Ohyama, K., Sharp, L.Z., and Kajimura, S. (2013). EHMT1 controls brown adipose cell fate and thermogenesis through the PRDM16 complex. *Nature* 504, 163–167.
- Papasaikas, P., Tejedor, J.R., Vigevani, L., and Valcárcel, J. (2015). Functional splicing network reveals extensive regulatory potential of the core spliceosomal machinery. *Mol. Cell* 57, 7–22.
- Perales, R., and Bentley, D. (2009). “Cotranscriptionality”: the transcription elongation complex as a nexus for nuclear transactions. *Mol. Cell* 36, 178–191.
- Rathert, P., Dhayalan, A., Murakami, M., Zhang, X., Tamas, R., Jurkowska, R., Komatsu, Y., Shinkai, Y., Cheng, X., and Jeltsch, A. (2008). Protein lysine methyltransferase G9a acts on non-histone targets. *Nat. Chem. Biol.* 4, 344–346.
- Saint-André, V., Batsché, E., Rachez, C., and Muchardt, C. (2011). Histone H3 lysine 9 trimethylation and HP1 γ favor inclusion of alternative exons. *Nat. Struct. Mol. Biol.* 18, 337–344.
- Salton, M., Voss, T.C., and Misteli, T. (2014). Identification by high-throughput imaging of the histone methyltransferase EHMT2 as an epigenetic regulator of VEGFA alternative splicing. *Nucleic Acids Res.* 42, 13662–13673.
- Schaefer, A., Sampath, S.C., Intrator, A., Min, A., Gertler, T.S., Surmeier, D.J., Tarakhovsky, A., and Greengard, P. (2009). Control of cognition and adaptive behavior by the GLP/G9a epigenetic suppressor complex. *Neuron* 64, 678–691.
- Schor, I.E., Rascovan, N., Pelisch, F., Alló, M., and Kornblhtt, A.R. (2009). Neuronal cell depolarization induces intragenic chromatin modifications affecting NCAM alternative splicing. *Proc. Natl. Acad. Sci. USA* 106, 4325–4330.
- Schor, I.E., Fiszbein, A., Petrillo, E., and Kornblhtt, A.R. (2013). Intragenic epigenetic changes modulate NCAM alternative splicing in neuronal differentiation. *EMBO J.* 32, 2264–2274.
- Shi, Y., Desponts, C., Do, J.T., Hahn, H.S., Schöler, H.R., and Ding, S. (2008). Induction of pluripotent stem cells from mouse embryonic fibroblasts by Oct4 and Klf4 with small-molecule compounds. *Cell Stem Cell* 3, 568–574.
- Shukla, S., Kavak, E., Gregory, M., Imashimizu, M., Shutinoski, B., Kashlev, M., Oberdoerffer, P., Sandberg, R., and Oberdoerffer, S. (2011). CTCF-promoted RNA polymerase II pausing links DNA methylation to splicing. *Nature* 479, 74–79.
- Sims, R.J., 3rd, Millhouse, S., Chen, C.F., Lewis, B.A., Erdjument-Bromage, H., Tempst, P., Manley, J.L., and Reinberg, D. (2007). Recognition of trimethylated histone H3 lysine 4 facilitates the recruitment of transcription postinitiation factors and pre-mRNA splicing. *Mol. Cell* 28, 665–676.
- Subbanna, S., Shivakumar, M., Umapathy, N.S., Saito, M., Mohan, P.S., Kumar, A., Nixon, R.A., Verin, A.D., Psychoyos, D., and Basavarajappa, B.S. (2013). G9a-mediated histone methylation regulates ethanol-induced neurodegeneration in the neonatal mouse brain. *Neurobiol. Dis.* 54, 475–485.
- Surani, M.A., Hayashi, K., and Hajkova, P. (2007). Genetic and epigenetic regulators of pluripotency. *Cell* 128, 747–762.
- Tachibana, M., Sugimoto, K., Nozaki, M., Ueda, J., Ohta, T., Ohki, M., Fukuda, M., Takeda, N., Niida, H., Kato, H., and Shinkai, Y. (2002). G9a histone methyltransferase plays a dominant role in euchromatic histone H3 lysine 9 methylation and is essential for early embryogenesis. *Genes Dev.* 16, 1779–1791.
- Tachibana, M., Matsumura, Y., Fukuda, M., Kimura, H., and Shinkai, Y. (2008). G9a/GLP complexes independently mediate H3K9 and DNA methylation to silence transcription. *EMBO J.* 27, 2681–2690.
- Tilgner, H., Knowles, D.G., Johnson, R., Davis, C.A., Chakraborty, S., Djebali, S., Curado, J., Snyder, M., Gingras, T.R., and Guigó, R. (2012). Deep sequencing of subcellular RNA fractions shows splicing to be predominantly co-transcriptional in the human genome but inefficient for lncRNAs. *Genome Res.* 22, 1616–1625.
- Vargas, D.Y., Shah, K., Batish, M., Levandoski, M., Sinha, S., Marras, S.A., Schedl, P., and Tyagi, S. (2011). Single-molecule imaging of transcriptionally coupled and uncoupled splicing. *Cell* 147, 1054–1065.
- Wada, S., Ideno, H., Shimada, A., Kamiunten, T., Nakamura, Y., Nakashima, K., Kimura, H., Shinkai, Y., Tachibana, M., and Nifufi, A. (2015). H3K9MTase G9a is essential for the differentiation and growth of tenocytes in vitro. *Histochem. Cell Biol.* 144, 13–20.
- Wierda, R.J., Goedhart, M., van Eggermond, M.C., Muggen, A.F., Miggelbrink, X.M., Geutskens, S.B., van Zwet, E., Haasnoot, G.W., and van den Elsen, P.J. (2015). A role for KMT1c in monocyte to dendritic cell differentiation: Epigenetic regulation of monocyte differentiation. *Hum. Immunol.* 76, 431–437.